On the Plausibility of Drying in the Sahel Associated with Global Warming

Isaac M. Held[1]

Jian Lu[2]

[1]**Geophysical Fluid Dynamics Laboratory/NOAA, Princeton NJ**

[2]**UCAR Visiting Scientist, GFDL/NOAA**

October 6, 2006

Submitted to J. Climate

Corresponding author address: Isaac M. Held, Geophysical Fluid Dynamics Laboratory, P.O.Box 308, Princeton, NJ 08542.

Abstract:

The Geophysical Fluid Dynamics Laboratory's CM2.1 climate model simulates strong drying in the Sahel in response to increases in greenhouse gases. This response is not sensitive to the detailed spatial structure of the oceanic warming; the atmosphere/land component of this model, AM2.1, simulates a drying of the Sahel in response to a uniform warming of the ocean surface. We train a simple linear statistical model using the 20th century co-variability of Sahel rainfall and Atlantic and Indian sea surface temperatures in both the fully-coupled CM2.1 and in AM2.1 running over observed sea surface temperatures. This statistical model predicts the drying in the coupled model's 21st century simulations. Comparison with the regressions obtained with observed precipitation and temperature fields supports the plausibility of a drying response over the Sahel as a consequence of increasing greenhouse gases.

Repeating this procedure with a model that predicts a much wetter Sahel in the future, MIROC2.3(medres), the linear statistical fit trained on the models' 20th century correctly predicts the sign of the model's Sahel rainfall response in the 21st century, but the magnitude of the response is underestimated. The regression explains a much smaller fraction of the variance in the MIROC model as compared to CM2.1. A statistical model capable of reliably predicting a GCM's 21st century Sahel rainfall from its SST-rainfall co-variability in the 20th century would provide a basis for a more definitive evaluation of model projections.

1. Introduction

There is a consensus that the dramatic multi-decadal variability of Sahel rainfall in the 20th century is strongly linked with changes in sea surface temperatures (SSTs). It has also been clear since the work of Folland et al., (1986), Palmer (1986) and Rowell et al., (1995), that the interhemispheric gradient in SSTs is centrally important for the Sahel, with greater warmth in the Northern Hemisphere favoring increased rainfall. However, Held et al (2005) describes a model that dries the Sahel in response to uniform warming of SSTs. Needless to say, a drying tendency in response to a uniform warming of ocean temperature has import for the response to increasing greenhouse gases (see also Giannini et al., 2003). The models analyzed by Held et al., GFDL's CM2.0 and CM2.1 (Delworth et al., 2005), dry the Sahel in the 21st century in the standard scenarios utilized by the Fourth Assessment (AR4) of the Intergovernmental Panel on Climate Change (IPCC). The magnitude of this drying is an outlier among the models archived by the Program in Model Diagnosis and Intercomparison[1] (PCMDI), many of which, in fact, project moistening of the Sahel in the 21st century (Hoerling et al, 2006; Biasutti and Giannini, 2006). Our intention in this note is to provide further information with which to judge the plausibility of the severe drying predicted by the GFDL CM2 models.

We present a simple regression analysis of the SST-Sahel rainfall relationship in observations, in CM2.1, and in the atmosphere/land component of this model when run over observed SSTs. The simplicity of the analysis may seem naïve. We choose only two predictors, North Atlantic and Indian Ocean SSTs. Others, starting with Folland, et al.

[1] http://www-pcmdi.llnl.gov/ipcc/about_ipcc.php

(1986), have performed more comprehensive regression analyses of African rainfall/SST relationships, often starting with an EOF decomposition of the SST field. We have opted for simplicity to ease the comparison of a variety of models, and also because we believe that the assumption of linearity on which the analysis is based is unlikely to be accurate enough, for precipitation anomalies of the magnitude observed over the Sahel, to warrant a very detailed linear analysis. The hypothesis underlying our choice of predictors is that there are (at least) two distinct mechanisms in play, which can loosely be thought of as ITCZ-displacement associated with the change in gradient, and stabilization of the troposphere associated with warming of the tropical oceans (e.g., Chiang and Sobel, 2002).

Questions have been raised concerning the strength and even the direction of the causal link between SST and convection over the Indian Ocean (see the discussion in Tompkins, 2001). The Indian Ocean SST predictor used in the following analysis, and the North Atlantic predictor for that matter, may, in part, be proxies for SST patterns with which they are strongly correlated on the decadal and longer time scales on which we focus here.

In Section 2 we describe results from a regression analysis of observations. This analysis illustrates the difficulty of extracting the response to uniform warming from the much larger effects of changing SST gradients in the 20th century. We then describe a similar analysis of AM2.1 running over observed SSTs in Section 3 and the coupled model

CM2.1 in Section 4. In Section 5 we briefly contrast these results with those obtained for a model that projects a much wetter, rather than drier, Sahel in the 21st century.

2. Observations

Our definitions of the Sahel (land areas within 10-20N, 20W-40E), an Indian Ocean box (25S-8N, 55E-95E), and a North Atlantic box (10N-42N, 62W-22W) are illustrated in Fig. 1. The Sahel so defined extends further eastward than the area traditionally given this designation. On the inter-decadal time scales of most interest here there is relatively little sensitivity to the precise definition of these boxes. Even reducing the size of the Atlantic box to a tropical one from (10N-20N) does not change our qualitative conclusions.

We define *P* to be the summer (July-Aug-Sept) rainfall averaged over the Sahel, after dividing by the mean over the years 1901-2002 and then subtracting unity. Observed values are taken from the CRU_TS_2.1 gridded data set[2] (New et al., 2000), and are displayed in Fig. 2. We define *I* to be the SST in the Indian Ocean box for each June-July-Aug season, with the mean over this same time period removed. (The SST averaging period is displaced one month earlier than the precipitation period, with the idea that the atmosphere takes several weeks to respond to the SST pattern, but the results are not sensitive to this difference.) We define *A* analogously for the North Atlantic Ocean box (10N-42N, 62W-22W). We use the HadISST_1.1 dataset[3] (Rayner, et al., 2003) for SSTs. The evolution of these two indices, and the difference between them, are

[2] http://www.cru.uea.ac.uk/~timm/grid/CRU_TS_2_1.html
[3] http://badc.nerc.ac.uk/data/hadisst

also plotted in Figure 2. Casual inspection of the figure is sufficient to motivate the hypothesis that the decadal variations in Sahel rainfall are related to the temperature difference $D = A - I$.

In addition to the overall warming trend in both basins, the North Atlantic warmed with respect to the Indian from the 20's to the 50's and then cooled till the 70's-80's, after which it warmed once again. This relative variation is caused by departures of the Indian from linear warming as well as by the Atlantic multi-decadal variations. For a better sense of the co-variation of these two indices, we plot D vs. I in Fig. 3, after smoothing with a 9-year running mean for clarity. If the system were warming uniformly in space the timeline would move horizontally to the right. The contour lines are explained below.

Regressing P against A and I, one obtains

$$P = \alpha_I I + \alpha_A A = \alpha_U I + \alpha_A D$$
$$\alpha_U \equiv \alpha_I + \alpha_A$$
$$D = A - I.$$

Using unfiltered seasonal means, the result is α_I = - 0.40 and α_A = + 0.27, or α_U = - 0.13. Using instead 5yr running means, the values are α_I = - 0.50 and α_A = + 0.35, or α_U = - 0.15. Some sensitivity to time filtering is expected if the patterns of SST variability change as a function of frequency and if the dominant patterns at different frequencies project differently on the I and A indices. Using 1-2-3-2-1 smoothing or the 9yr running means plotted in Fig 3 results in relatively small change to the 5yr running mean results.

The decrease in precipitation in response to an increase in Indian Ocean temperature (α_I < 0), and the increase in response to an increase in North Atlantic Ocean temperature (α_A > 0), are as expected from previous work (Palmer, 1986; Rowell, et al., 1995; Bader and Latif, 2003; Lu and Delworth, 2005). Our primary focus is on the sign of α_U, with negative values implying drying in response to uniform warming in this two-parameter space. There is a hint that the value of α_U is less sensitive to the time filtering than are the values of α_A and α_I individually. The best fit values using 5yr running means are used to draw the contours in Fig. 3, from which one can read off the Sahel rainfall estimate from the position of the system in the (*I*,*D*) plane.

The time series from the best fit is compared with the data in Fig. 4a, again using 5yr means. The variance explained is 84%. Also shown is the contribution to this fit from the term $\alpha_U I$ only. Fig 4b shows the result of a one-parameter fit, using only the single predictor *D*. The variance explained in this case is 72%, with α_A = 0.40. To test the significance in the reduction in variance in the 2-paramter fit, while avoiding the necessity of estimating effective degrees of freedom (Ebusizaki, 1997), we take the residual from the one-parameter fit, compute its discrete Fourier transform, then randomize the phase of each Fourier component holding its amplitude fixed. The original residual is replaced by this randomized residual and the 2-parameter fit recomputed. Repeating this procedure 1000 times, using the 5yr running mean time series, we find a marginal significance (p ~ 0.09) to the reduction in variance in the two-parameter over the one-parameter fit. On the other hand, randomizing the phases in the

residuals from the two-parameter fit produces surprisingly small error bars on the regression coefficients with a negligible fraction of cases with positive α_U .

Much of the modest improvement in the fit upon introduction of α_U occurs in the early part of the record. When we repeat the regression using data from only the last half of the 20th century, the result is a smaller value of α_U (see Figure 5). More generally, downweighting the earlier part of the record when minimizing the residual variance reduces the magnitude of α_U and increases the magnitude of α_A.

There is evidently a tradeoff between sensitivity to temperature gradient, α_A, and sensitivity to uniform warming, α_U . A good fit is obtained with a large value of α_A = 0.40 with no contribution from the uniform warming component, but as good a fit, a bit better possibly, is obtained with smaller value of α_A = + 0.35 accompanied by α_U = - 0.15. We cannot make a strong case for the latter alternative, given its sensitivity to the early part of the 20th century record and the marginal significance of the reduction in explained variance. On the other hand, a reduction in rainfall as large as 15% per degree uniform warming seems fully consistent with these observations.

3. AM2.1 run over observed SSTs

Lu and Delworth (2005) describe a 10-member ensemble of integrations of AM2.0 (the atmospheric/land component of CM2.0), running over observed SSTs for the period 1950-2000. These integrations have now been complemented by a 10 member ensemble of integrations using AM2.1 over the extended period from 1865 to 2005. All forcings

(well-mixed greenhouse gases, aerosols, ozone, land use, insolation) are held fixed at 1860 values, and there are no volcanoes. The seasonal mean Sahel rainfall produced by this model is compared with observations in Fig. 6, with 5yr smoothing. The median, as well as the range of the 10-member ensemble, are plotted as fractional changes from the mean over the century. On average, AM2.1 in this framework overestimates rainfall in this Sahel box by 12%.

The quantitative agreement in Fig. 6 speaks to the model's ability to simulate the response of Sahelian rainfall to SST variability. The model captures not only the drying from the 50s to the 80s, as described for AM2.0 in Lu and Delworth (2005), but also the increase in rainfall in the first part of the century. Closer inspection reveals interesting discrepancies as well (the inability to capture the driest years in the early 1980's, and the overprediction of very wet years in the 1930's). Since the SST input into this model and the precipitation data set are independent, the model fit also indirectly increases confidence in the basic features of the early 20^{th} century components of both sets of observations. A 10 member ensemble has also been generated with the same SST as prescribed but with forcing varying in time as in the CM2.1 all-forcing simulations. The results closely match those in Fig. 6. Once one has specified the SSTs, the forcing has only a small effect on Sahel rainfall in this model.

Repeating the regression analysis used on the observations, but with the precipitation generated by each of the 10 ensemble members, the result are the red dots in Fig. 5. The large red dot is the mean. The similarity in the regression coefficients implies that the

relative importance of the temperature gradient effect and the effect of uniform warming are comparable to that displayed in Fig. 4a.

Of course, with the GCM we can manipulate the SSTs directly to separate the effects of Atlantic and Indian Ocean SSTs as well as test for linearity. Some experiments of this type have been described in Lu and Delworth (2005), and additional information will be provided in a forthcoming paper. As described in Held et al (2005), , we have compared an integration of AM2.1 over observed climatological (seasonally varying) SSTs and sea ice with an integration in which the SSTs are uniformly increased by 2K, providing a direct test of the claim that α_U provides an estimate of the response to uniform warming. Sahel rainfall is reduced in this case by 18%/K. The closeness of this result to that obtained in the regression analysis is coincidental; we find significant nonlinearity (with an even larger response) when we cool the model by 2K, for example. But the qualitative result suggested by the regression analysis is confirmed by this direct manipulation of the model.

4. CM2.1

An ensemble of 5 full-forcing simulations for the 20th century exist using the GFDL coupled model CM2.1, as described in Knutson, et al. (2006). We have regressed the 5-year running mean Sahel rainfall in each of these integrations with the Atlantic and Indian temperature indices A and I simulated in the same integration. We have also repeated this process using the ensemble mean temperature indices and rainfall. The ensemble averaging emphasizes the forced response, and one expects the temperature

variations in the forced response, dominated by greenhouse gases and aerosols, to have a different spatial structure than the models internal variability, and these different structures might in turn project differently on our SST indices. There is no reason, in general, to expect the regression based on the ensemble mean to be close to the ensemble mean of the regression coefficients obtained from the individual realizations. The results are displayed in Fig 5, as the blue dots, the larger dot being the result of the regression on the ensemble means.

The result using the ensemble mean evolution is (α_I, α_A) = (-0.32, +0.20), or α_U = - 0.12. or a 12% drying per degree of uniform warming. Using individual realizations, the values for α_U congregate between -0.05 and -0.2, with all values negative and a mean value similar to that obtained using the ensemble mean as input into the regression. However, the value of α_A is smaller in each individual realization than when using the ensemble mean, and substantially smaller than in the observations. This difference between CM2.1 and AM2.1 run over observed SSTs could be due to biases in the coupled model, causing the convection zones to shift (especially over the Atlantic – see Delworth, et al (2006)) thereby modifying the models sensitivity to SST anomalies. Or it could be related to the limitations involved in mimicking fully coupled model simulations with atmospheric models running over prescribed SSTs (Douville, 2005). Or the regressions using individual realizations may be biased due to unrealistic aspects of the decadal variability in the coupled model. Some deficiencies in the coupled model in the Gulf of Guinea region are described by Cook and Vizy (2006).

Using the linear fit to the ensemble mean, we predict the rainfall in the 21st century, using the temperature changes simulated by the same model for each of the B1, A1B, and A2 scenarios. The predictions, shown in Figure 7, capture the trends rather accurately. Also captured is a rather sharp recovery at the end of the 20th century. While there may be some physical meaning to this recovery, we believe that its sharpness is artificial due abrupt changes in the aerosol concentrations between the 20th century integrations and the scenario runs for the 21st century. While this feature is related to changes in the gradient *D*, the bulk of the 21st century drying trend is due to the response to uniform warming, $\alpha_U I$.

If we use the ensemble mean of the regression coefficients for this purpose, rather than the regression coefficients from the ensemble mean, the fit over the 20th century is not as precise, but the 21st century evolution is similar because the mean value of α_U is very close to that obtained by fitting the ensemble mean.

The 20th century ensemble mean evolution shown in Fig. 7 is dominated by a steady negative trend, and bears little resemblance to the observed time series, although trends computed over the 20th century are comparable to those in the data (Held et al., 2005). The evolution of the ensemble mean of the CM2.1 20th century integrations in the *(D,I)* plane is displayed in Fig. 8a along with the observations. A single realization (run 3) that compares most favorably with the observed evolution is plotted in Fig. 8b. The ensemble mean shows a weak cooling of the Atlantic with respect to the Indian of only 0.1- 0.2K, mostly occurring from 1950-1970. The individual realization shown has SST variability

only slightly smaller than that observed and shows more recovery than does the ensemble mean in recent decades. For a comparison of the Sahel rainfall in individual realizations of both CM2.0 and CM2.1, see Held et al. (2005).

In Fig. 9, we plot the 20th century ensemble mean evolution once again (in green), but also shown (in blue) is one realization of the A1B scenario for the period 2000-2060 . The contours correspond to the best fit regression to the coupled model used in generating Fig. 7. In the 20th century, the regression implies that the drying observed in the ensemble mean model is in roughly equal parts due to the uniform component of the warming and to the cooling of the Atlantic with respect to the Indian. In the first half of the 21st century in this model projection, the North Atlantic warms faster than the Indian, helping to preventing the Sahel from drying in the model (cf. Fig. 7b). Later in the century warming becomes more uniform and the drying more rapid.

Also shown in Fig. 9 (in red) is the ensemble mean of the evolution of 6 integrations in which the only evolving forcing is the greenhouse gases. In three of these integrations, only the well-mixed greenhouse gases are considered, while in the other 3 both stratospheric and tropospheric ozone are varied as well, but we have no evidence that the latter are of significance for African rainfall, so we combine both sets of runs here to increase the ensemble size. These runs are warmer than the full-forcing runs in the early 20th century, primarily due to the absence of volcanic forcing. They show less cooling of the N. Atlantic with respect to the Indian in the second half of the century, primarily due to the absence of an aerosol effect. The effect of the non-greenhouse gas forcing in the

(D,I) plane is both to decrease *D* and decrease *I*, which have opposite effects on Sahel rain in the model. These plots are somewhat sensitive to the boundaries of the Atlantic box, so we focus on only the broadest features. Experiments with aerosol forcing only show a 5-10% reduction in the Sahel rainfall when computing linear trends over the century, accounting for roughly half of the trend in the model's 20th century simulation. For additional evidence for the aerosol effect on Sahel rainfall, see Rotstayn and Lohmann (2002) as well as Biasutti and Giannini (2006).

The models described do not take into account changes in dust aerosol that could potentially feed back onto African rainfall through either local effects over land or through changes in Atlantic SSTs

5. The MIROC model

Several of the models in the PCMDI/AR4 database project increasing rainfall in the Sahel, rather than the drying seen in CM2.1 (Hoerling et al, 2006; Biasutti and Giannini, 2006). The MIROC3.2(medres) model[4] (developed by the Center for Climate System Research at the University of Tokyo, the National Institute for Environmental Studies, and the Frontier Research Center for Global Change) produces the largest increase in precipitation in this ensemble of models, so it is of interest to contrast it with CM2.1.

Fig. 10 shows the 20th century simulation for July-August-September Sahel rainfall in MIROC_medres and the projection using the A1B scenario. In each case, we have

[4] http://www.ccsr.u-tokyo.ac.jp/kyosei/hasumi/MIROC/tech-repo.pdf

averaged over three of the realizations made available in the archive. The future projection is dramatically different from that in CM2.1, with an increase in precipitation of ~50% projected for the A1B scenario by the end of the century. There is a small drying trend in the 20th century in the ensemble mean, and individual realizations can be found that agree with the observations about as well as the realizations of CM2.1 that provide the best fit. The sharp change in behavior near the turn of the century is most likely attributable to aerosol forcing balancing the response to greenhouse gases in the 20th century.

Just as for CM2.1, we have used the 20th century simulations to regress Sahel precipitation against North Atlantic and Indian Ocean temperatures, once again using 5ry running means. The results for three 20th century realizations, and from a regression performed on the ensemble mean of these three runs, have been plotted as open diamonds in Figure 5. There is considerable scatter, but typically the increase in rainfall in response to North Atlantic warming is larger than the decrease to the Indian warming, so that α_U is positive. Using the regression based on the ensemble mean, one obtains the prediction shown in Fig. 10, which is for an increase in precipitation, but only ~30% of that realized in the model. This increase in precipitation is partly due to the fact that α_A is slightly larger than α_I in the regression, but also because the warming of the North Atlantic is larger than that of the Indian Ocean. If one uses the regression coefficients from the realization that produces the largest value of α_U, the fit would be better. The variance explained in the 20th century training period (21% using the ensemble mean simulation and only 12% on average for the individual realizations) is substantially

smaller than that in CM2.1 (64% for the ensemble mean and 36% on average for the realizations), which in turn, is smaller than the variance explained using the one realization of the observations (84%). It may be that alternative predictors, or a larger number of predictors, would provide a more convincing fit to the Sahel rainfall in the MIROC model and a more quantitative prediction of its 21st century trend.

The simple two-parameter fit described here does seem to capture the qualitative difference between 21st century projections in these two models, although it provides a quantitative fit only for the GFDL model. One is tempted to use the comparison with the observed regression coefficients to judge which model is more reliable. Fig. 5 does indicate that the regression of Sahel rain and SSTS in the GFDL CM2.1 model resembles the observed regression more closely than MIROC3.2(medres). However, the sensitivity of the observed regression to the exclusion of the first part of the 20th century reduces our confidence in this conclusion. Also, we cannot exclude the possibility that a regression with other predictors, that fits the MIROC model better, would show improved agreement with observations as well.

6. Discussion and Conclusions

GFDL's CM2.1 coupled model predicts dramatic drying in the Sahel in the 21st century. A simple multiple regression analysis of Sahel rainfall against North Atlantic and Indian SSTs provides useful checks on the realism of the model. The comparison with observed regressions increases the plausibility of this drying response in the Sahel, although it is not definitive.

Sahel rainfall can be affected by a variety of factors, including changes in interhemispheric gradients in SSTs that influence the latitude of the ITCZ, and factors that affect tropical tropospheric temperatures, thereby stabilizing or destabilizing convection over the Sahel. Qualitatively at least, the gradient between the Atlantic and the Indian ocean SSTs ($D = A - I$) can potentially be thought of as measuring the ITCZ displacement effect, and the Indian SSTs (I) in isolation as measuring the tropospheric stabilization effect. The qualitative character of these factors, when considered in isolation, may be relatively robust across models. The lack of robustness in the model projections for Sahel rainfall may in part reflect variations across models in the relative magnitude of these two effects.

The regression analysis using observed SSTs and rainfall does not provide a persuasive quantitative estimate of the response to I, holding D fixed, although the best fit yields a negative value, implying drying in response to uniform warming. This analysis does indicate that the existence of a drying in response to uniform warming as large as 15%/K cannot be ruled out by the observations.

The atmospheric/land component of CM.1 (AM2.1) provides an excellent simulation of interdecadal variations in Sahel rainfall throughout the 20th century when forced with observed SSTs. The regression analysis suggests that the rainfall/SST relationships, and, by inference, the ITCZ displacement and tropospheric stabilization effects, may be realistically balanced in the atmospheric model.

The regression analysis of the coupled model (CM2.1) indicates that Sahel rainfall in the model is insufficiently sensitive to interhemispheric SST gradients, and that this insensitivity likely reduces the internal variability of Sahel rainfall in the coupled model, as well as the model's response to aerosol forcing. However, the regression suggests that the model's response to uniform warming is comparable to, and possibly weaker than, that in the observations and in the fixed SST model.

The regression analysis described with observations only, with Sahel rainfall simulated by the atmospheric/land model run over observed SSTs, and with the freely running CM2.1 coupled model, all generates a drying in response to uniform warming of SSTs. When we check this prediction with a +2K uniform perturbation in the SSTs in the atmosphere/land model, the drying is confirmed, as described in Held, et al (2005). When we use the regression coefficients fit to the coupled model's 20th century evolution to predict the 21st century evolution in each of the A2, A1B, and B1 scenarios, the drying trends are accurately captured.

To determine if this regression analysis can predict the future of a model that simulates a wetter Sahel as well as it predicts the drying response in CM2.1, we examine the results from the MIROC3.2(medres) model. The result is moderately encouraging in that the resulting regression, trained on the models 20th century, does predict a wetter Sahel in the future. But the magnitude of the increase in precipitation is smaller than that in the MIROC model. It would be interesting to see if there exist better statistical models more

capable of predicting the future of various models in the PCMDI/AR4 archive from their 20th century variability.

Ideally, judgment as to the plausibility of CM2's projections for the Sahel should be based on a dynamical understanding of why this model differs from most other models. In the absence of a clear dynamical explanation that would form the basis for a more definitive evaluation, we rely on statistical tests against observations of the sort described here. Our analysis uncovers no clear deficiencies in the model that would argue for eliminating this model's projections for the Sahel as an unreliable outlier among the ensemble of projections from the world's climate models. On the contrary, we believe that this analysis increases the plausibility of CM2's projection of a drier Sahel in response to increasing greenhouse gases.

Acknowledgements:

We thank Tom Delworth, Tom Knutson, Michela Biasutti, Alessandra Giannini, and Adam Sobel for helpful conversations on the topic of African climate change, Andrew Wittenberg for helpful advice on statistical significance testing, and the contribution of V. Ramaswamy and Dan Schwarzkopf for running the aerosol-only and greenhouse-gas only simulations of CM2.1. We also acknowledge the MIROC development group for providing their data for analysis, the Program for Climate Model Diagnosis and Intercomparison (PCMDI) for collecting and archiving the model output, and the JSC/CLIVAR Working Group on Coupled Modelling (WGCM) for organizing the model data analysis activity. The multi-model data archive is supported by the Office of

Science, U.S. Department of Energy. Jian Lu was supported by the Visiting Sceintist program of the University Corporation for Atmospheric Research.

References:

Bader, J. and M Latif, 2003: The impact of decadal-scale Indian Ocean sea surface temperature anomalies on Sahelian rainfall and the North Atlantic Oscillation. *Geophys. Res. Letters*, **30**(22), 2169, doi:10.1029/2003GL018426.

Biasutti, M., and A. Giannini, 2006: Robust Sahel drying in response to late 20th century forcings. *Geophys. Res. Letters*, **10**, 1029/2006GRL026067**.**

Chiang, J. C. H., Sobel, A. H., 2002: Tropical Tropospheric Temperature Variations Caused by ENSO and Their Influence on the Remote Tropical Climate. *J. Climate*, **15**, 2616-2631.

Cook, K. H. and E. K. Vizy, 2006: Coupled model simulations of the West African Monsoon system: Twentieth- and twenty-first-century simulations. *J. Climate*, **19**(15), 3681-3703.

Delworth, T. L., et al, 2006: GFDL's CM2 global coupled climate models. Part I: Formulation and simulation characteristics. *J. Climate*, **19**(5), 643-674.

Douville, H, 2005: Limitations of time-slice experiments for predicting regional climate change over South Asia. *Clim. Dynamics*, **24**(4), 373-391

Ebisuzaki, W., 1997: A method to estimate the statistical significance of a correlation when the data are serially correlated. *J. Climate*, **10**, 2147-2153.

Folland, C. K., T.N. Palmer, and D.E. Parker, 1986: Sahel rainfall variability and worldwide sea temperatures, 1901-85. *Nature*, **320**, 602-606.

Giannini, A., R.Saravanan, and P. Chang, 2003: Oceanic forcing of Sahel rainfall on interannual to interdecadal timescales. *Science*, **302**, 1027-1030.

Held, I. M., T. L. Delworth, J. Lu, K. L. Findell, and T. R. Knutson, 2005: Simulation of Sahel drought in the 20th and 21st centuries. *Proc. Nat. Acad. Sci.*, **102**(50), 17891-17896.

Hoerling, M.P., Hurrell, J. W., and Eischeid, 2006: Detection and Attribution of 20th Century Northern and Southern African Monsoon Change. *J. Climate*, **19**(16) 3989-4008.

Knutson, T. R., T. L. Delworth, K. W. Dixon, I. M. Held, J. Lu, V. Ramaswamy, M. D. Schwarzkopf, G. Stenchikov, and R. J. Stouffer, 2006: Assessment of twentieth-century regional surface temperature trends using the GFDL CM2 coupled models. *J. Climate*, **10**(9), 1624-1651.

Lu, J. and T. L. Delworth, 2005: Oceanic forcing of the late 20th century Sahel drought. *Geophys. Res. Letters*, **32**, L22706, doi:10.1029/2005GL023316.

New, M. G., M. Hulme, and P. D. Jones, 2000: Representing twentieth-century space-time climate variability. Part II: Development of 1901-1996 monthly grids of terrestrial surface climate. *J. Climate*, **13**, 2217-1138.

Palmer, T.N., 1986: Influence of Atlantic, Pacific, and Indian Oceans on Sahel Rainfall. *Nature*, **322**, 251-253.

Rayner, N. A.m D. E. Parker, E. B. Horton, C. K. Folland, L. V. Alexander, D. P. Rowell, E. C. Kent, and A. Kaplan, 2003: Global analyses of SST, sea-ice, and night marine air-temperature since the late nineteenth century. *J. Geophys. Res*, **108**(D14), 4407, doi:10.1029/2002JD002670, 2003

Rotstayn, L. D., and Lohmann, U., 2002: Tropical rainfall trends and the indirect aerosol effect. *J. Climate*, **14**, 2103-2116.

Rowell, D. P., C. K. Folland, N. M. Maskell, and N. M. Ward, 1995: Variability of summer rainfall over tropical Africa (1906-92): Observations and modelling. *Quart. J. Roy. Meteor. Soc.*, **121**, 669-704.

Tompkins, A. M., 2001: On the Relationship between tropical convection and sea surface temperature. *J. Climate*, **14**, 633-637

Figure Captions:

Figure 1: Areas over which the Sahel precipitation is averaged and over which SSTs are averaged in the Atlantic and Indian Oceans.

Figure 2: Time evolution of North Atlantic (*A*) and Indian (*I*) SSTs, the difference between the two (*D*=*A*-*I*), and Sahel rainfall (*P*), averaged over July-Aug-Sept, with no additional smoothing. SSTs in degrees C with mean over the 20th century removed; Sahel rainfall is percentage change from mean over the full century. SSTs from HADISST_1.1; rainfall from CRU_TS_2.1.

Figure 3: Evolution of the SSTs in the *(D,I)* plane, where $D = A - I$, A = North Atlantic and I = Indian, with 9 yr smoothing. Labels on the path indicate the center date of the 9 yr smoothing interval. Contours represent Sahel rainfall *P* predicted by the regression described in text.

Figure 4: Statistical fits to observed variations in Sahel rainfall. Black line in both figures is the observation Sahel rainfall *P(t)* with 5yr running mean. Left: Red line is two-parameter fit using observed 5ry running mean *A* and *I*. Blue line is the contribution to this fit from the uniform warming component, $\alpha_U I$. Right: Red line is one parameter fit using only $D = A - I$. Rainfall is normalized by its mean.

Figure 5. Plot of the regression coefficients. Large black dot: observed regression using the full 20th century. Smaller black dot: observed regression using only last 50 years of 20th century. Larger red dot: regression using the ensemble mean of the AM2.1 rainfall simulations. Small red dots: regressions using 10 individual AM2.1 simulations. Large blue dot: regression using ensemble mean CM2.1 full-forcing 20th century integrations. Small blue dots: regressions for 5 individual CM2.1 full-forcing 20th century simulations. Large diamond: regression using ensemble mean MIROC3.2(medres) full-forcing 20th century simulations. Small diamonds: regressions for individual MIROC full-forcing 20th century simulations.

Figure 6. Comparison of observed fractional variations in Sahel rainfall with simulation using atmosphere/land model running over observed SSTs. Black line is *P(t)* with 5yr running mean, normalized by the time mean. Red line is median of 10 realizations of AM2.1/LM2.1 running over observed SSTs. 5yr running mean smoothing is applied before plotting, and the model rainfall is normalized by its own time mean. Gray shading indicates the range of the 10 individual realizations.

Figure 7. B1(left); A1B(center); A2(right). Blue line is 5-yr running mean CM2.1 Sahel rainfall; red line is regression prediction. Before 2000, the blue line is the ensemble mean for CM2.1, on which the regression is trained.

Figure 8. Evolution in the *(D,I)* plane of the observations (black), ensemble mean CM2.1 all-forcing 20th century simulations (green on left), and an individual realization from this

ensemble (blue on right), all with 9yr smoothing and with the mean over the century removed.

Figure 9: Green line is ensemble mean evolution of CM2.1 20th century all-forcing runs with 9yr running mean (as in fig. 8). Blue line is one realization of the A1B scenario up to year 2060, with the 20th century ensemble and time mean removed. Red line is ensemble mean of 6 runs with greenhouse gas only forcing, as described in text. All curves are smoothed with 9yr running mean and normalized by subtracting the time mean of the ensemble mean of the CM2.1 all-forcing runs. (These are actually 11yr menas, have to redo this plot with 9yr means instead). Straight lines are percent change in Sahel rainfall predicted from linear regression on ensemble mean CM2.1 20th century all-forcing runs.

Figure 10: The ensemble mean Sahel rainfall projected by the MIROC3.2(medres) model, using the A1B scenario for the 21st century (solid line) and the result of the two-parameter fit trained with the 20th century rainfall and Atlantic and Indian SST variations (red line).

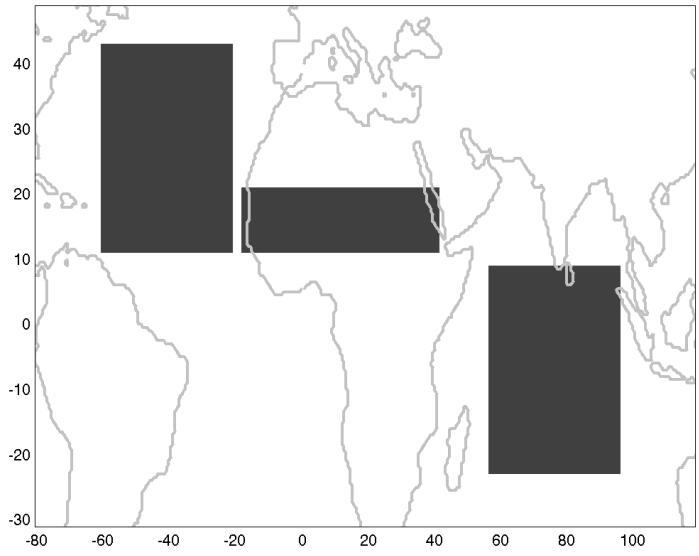

Figure 1: Areas over which the Sahel precipitation is averaged and over which SSTs are averaged in the Atlantic and Indian Oceans.

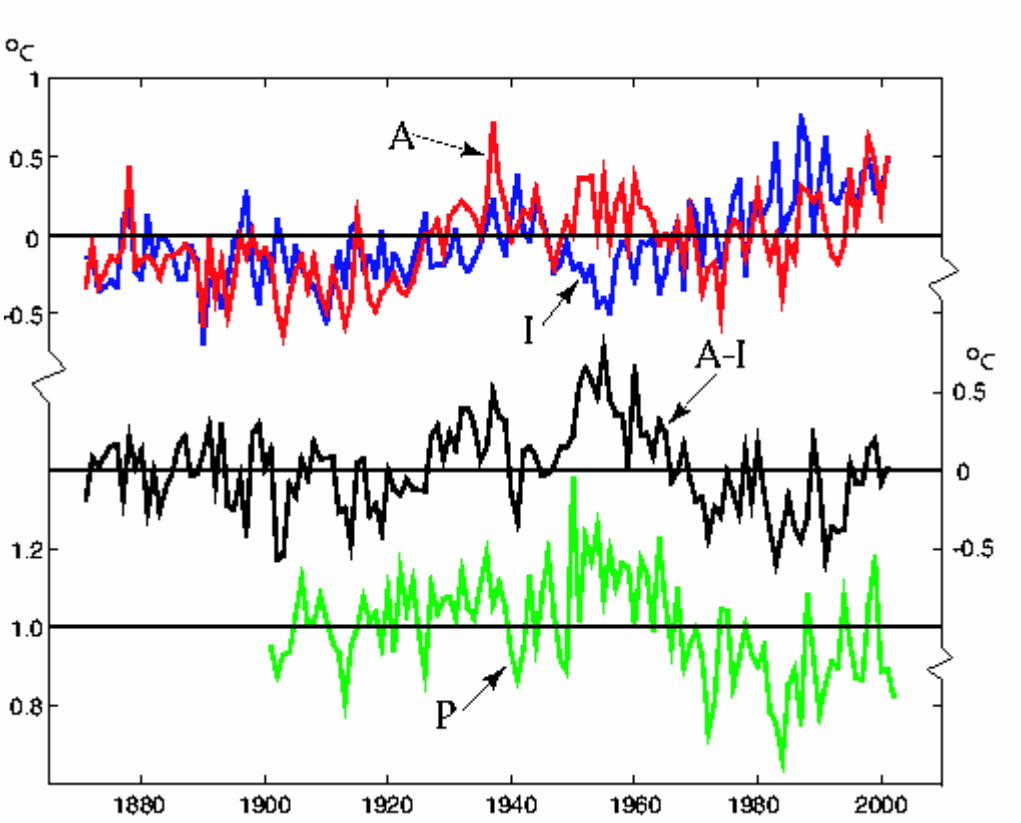

Figure 2: Time evolution of North Atlantic (A) and Indian (I) SSTs, the difference between the two (D=A-I), and Sahel rainfall (P), averaged over July-Aug-Sept, with no additional smoothing. SSTs in degrees C with mean over the 20th century removed; Sahel rainfall is percentage change from mean over the full century. SSTs from HADISST_1.1; rainfall from CRU_TS_2.1.

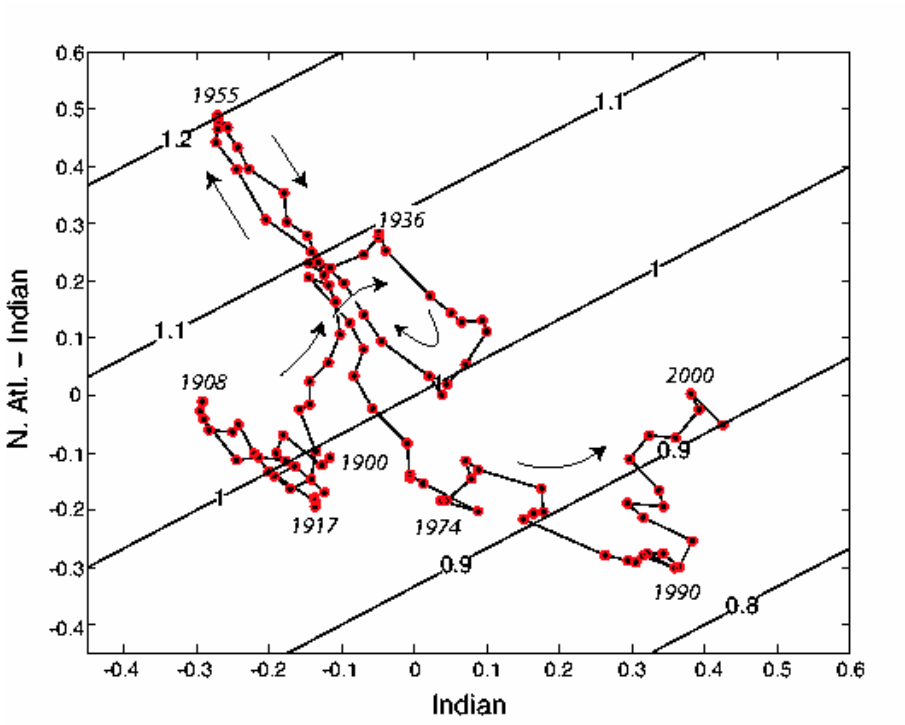

Figure 3: Evolution of the SSTs in the *(D,I)* plane, where $D = A - I$, A = North Atlantic and I = Indian, with 9 yr smoothing. Labels on the path indicate the center date of the 9 yr smoothing interval. Contours represent Sahel rainfall P predicted by the regression described in text.

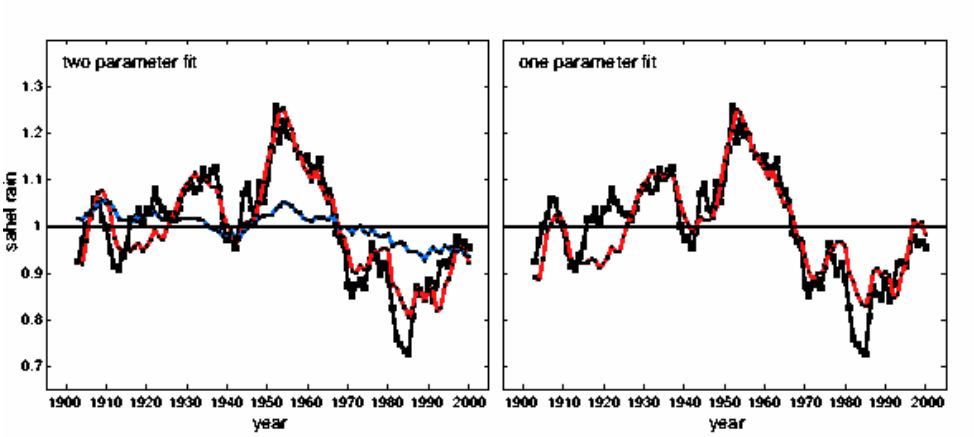

Figure 4: Statistical fits to observed variations in Sahel rainfall. Black line in both figures is the observation Sahel rainfall $P(t)$ with 5yr running mean. Left: Red line is two-parameter fit using observed 5ry running mean A and I. Blue line is the contribution to this fit from the uniform warming component, $\alpha_U I$. Right: Red line is one parameter fit using only $D = A - I$. Rainfall is normalized by its mean.

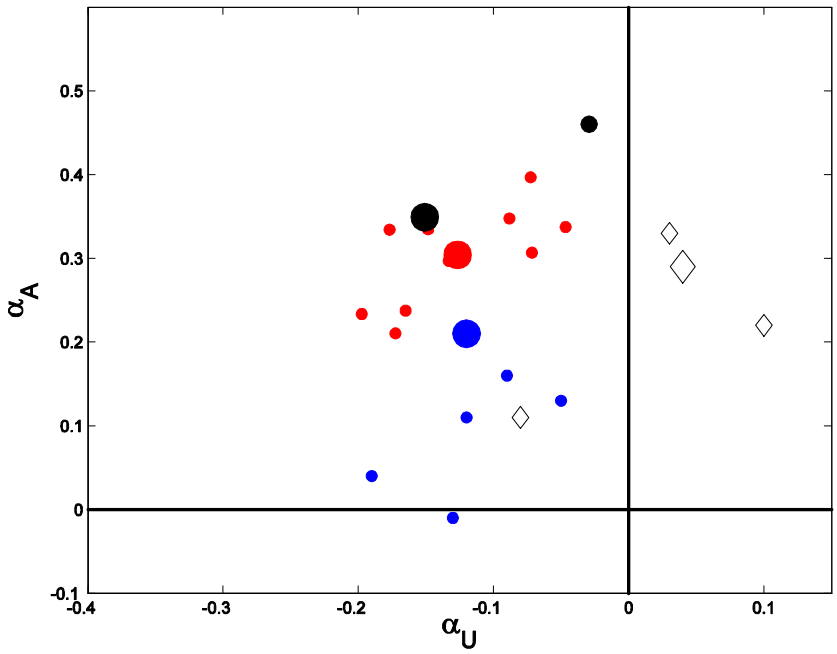

Figure 5. Plot of the regression coefficients. Large black dot: observed regression using the full 20th century. Smaller black dot: observed regression using only last 50 years of 20th century. Larger red dot: regression using the ensemble mean of the AM2.1 rainfall simulations. Small red dots: regressions using 10 individual AM2.1 simulations. Large blue dot: regression using ensemble mean CM2.1 full-forcing 20th century integrations. Small blue dots: regressions for 5 individual CM2.1 full-forcing 20th century simulations. Large diamond: regression using ensemble mean MIROC3.2(medres) full-forcing 20th century simulations. Small diamonds: regressions for individual MIROC full-forcing 20th century simulations.

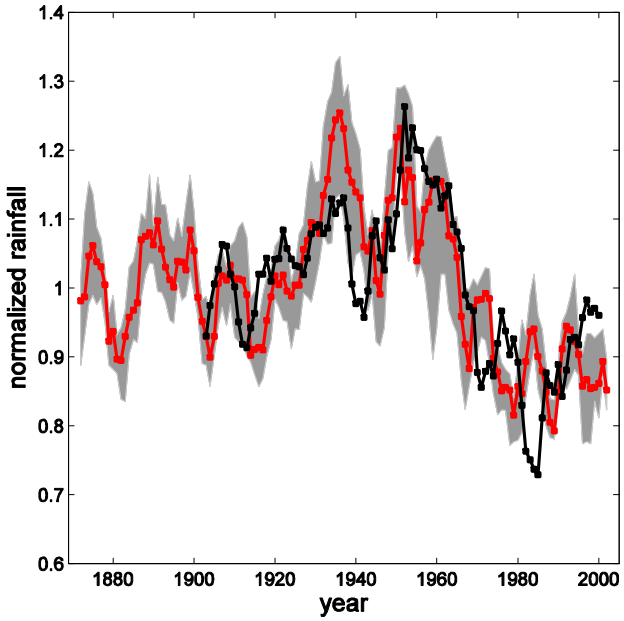

Figure 6. Comparison of observed fractional variations in Sahel rainfall with simulation using atmosphere/land model running over observed SSTs. Black line is *P(t)* with 5yr running mean, normalized by the time mean. Red line is median of 10 realizations of AM2.1/LM2.1 running over observed SSTs. 5yr running mean smoothing is applied before plotting, and the model rainfall is normalized by its own time mean. Gray shading indicates the range of the 10 individual realizations.

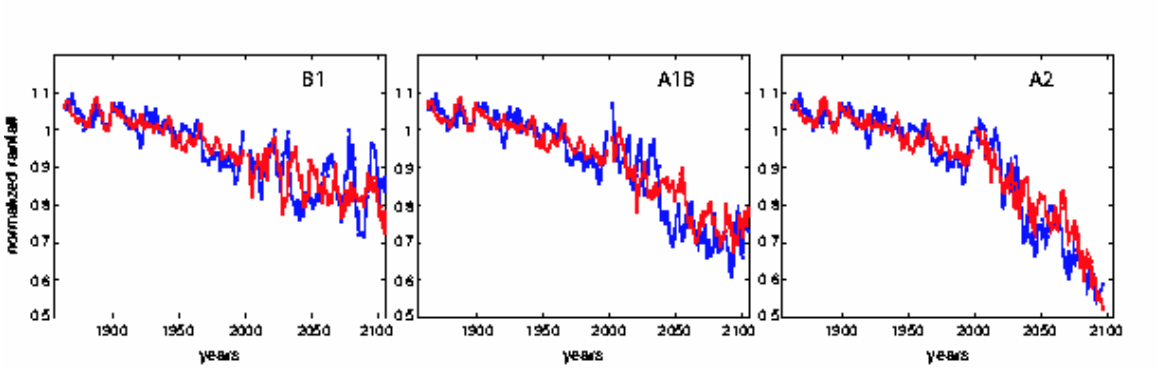

Figure 7: B1(left); A1B(center); A2(right). Blue line is 5-yr running mean CM2.1 Sahel rainfall; red line is regression prediction. Before 2000, the blue line is the ensemble mean for CM2.1, on which the regression is trained.

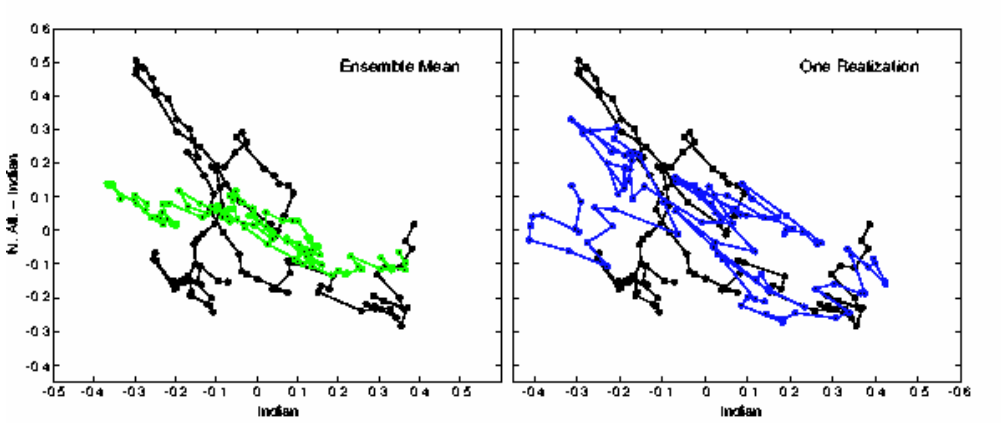

Figure 8: Evolution in the *(D,I)* plane of the observations (black), ensemble mean CM2.1 all-forcing 20th century simulations (green on left), and an individual realization from this ensemble (blue on right), all with 9yr smoothing and with the mean over the century removed.

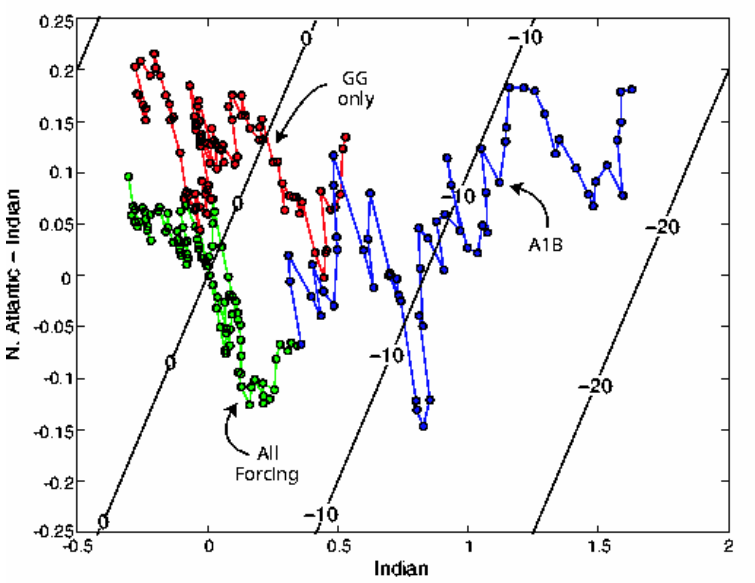

Figure 9: Green line is ensemble mean evolution of CM2.1 20th century all-forcing runs with 9yr running mean (as in fig. 8). Blue line is one realization of the A1B scenario up to year 2060, with the 20th century ensemble and time mean removed. Red line is ensemble mean of 6 runs with greenhouse gas only forcing, as described in text. All curves are smoothed with 9yr running mean and normalized by subtracting the time mean of the ensemble mean of the CM2.1 all-forcing runs. (These are actually 11yr menas, have to redo this plot with 9yr means instead). Straight lines are percent change in Sahel rainfall predicted from linear regression on ensemble mean CM2.1 20th century all-forcing runs.

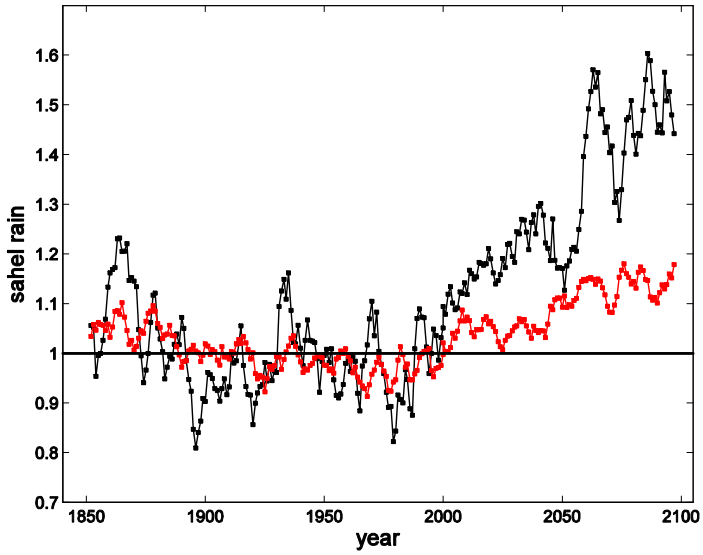

Figure 10: The ensemble mean Sahel rainfall projected by the MIROC3.2(medres) model, using the A1B scenario for the 21st century (solid line) and the result of the two-parameter fit trained with the 20th century rainfall and Atlantic and Indian SST variations (red line).